Aberrant hypomethylation-mediated *AGR2* overexpression induces an aggressive phenotype in ovarian cancer cells

HYE YOUN SUNG[1], EUN NAM CHOI[1], DAHYUN LYU[1],
AE KYUNG PARK[2], WOONG JU[3] and JUNG-HYUCK AHN[1]

[1]Department of Biochemistry, School of Medicine, Ewha Womans University, Seoul 158-710;
[2]College of Pharmacy, Sunchon National University, Jeonnam 540-742; [3]Department of Obstetrics and Gynecology, School of Medicine, Ewha Womans University, Seoul 158-710, Republic of Korea

Received February 6, 2014; Accepted March 30, 2014

DOI: 10.3892/or.2014.3243

Abstract. The metastatic properties of cancer cells result from genetic and epigenetic alterations that lead to the abnormal expression of key genes regulating tumor phenotypes. Recent discoveries suggest that aberrant DNA methylation provides cancer cells with advanced metastatic properties; however, the precise regulatory mechanisms controlling metastasis-associated genes and their roles in metastatic transformation are largely unknown. We injected SK-OV-3 human ovarian cancer cells into the perineum of nude mice to generate a mouse model that mimics human ovarian cancer metastasis. We analyzed the mRNA expression and DNA methylation profiles in metastasized tumor tissues in the mice. The pro-oncogenic anterior gradient 2 *(AGR2)* gene showed increased mRNA expression and hypomethylation at CpG sites in its promoter region in the metastatic tumor tissues compared with the cultured SK-OV-3 cells. We identified crucial cytosine residues at CpG sites in the *AGR2* promoter region. Treatment with the DNA methyltransferase inhibitor 5-aza-2'-deoxycytidine reduced the level of CpG methylation in the *AGR2* promoter and increased the level of *AGR2* expression. Next, we explored the functional role of *AGR2* in the metastatic transformation of SK-OV-3 cells. SK-OV-3 cells overexpressing *AGR2* showed increased migratory and invasive activity. Our results indicate that DNA methylation within the *AGR2* promoter modulates more aggressive cancer cell phenotypes.

Correspondence to: Professor Jung-Hyuck Ahn, Department of Biochemistry, School of Medicine, Ewha Womans University, 911-1 Mok-5-dong, Yangcheon-ku, Seoul 158-710, Republic of Korea
E-mail: ahnj@ewha.ac.kr

Professor Woong Ju, Department of Obstetrics and Gynecology, School of Medicine, Ewha Womans University, 911-1 Mok-5-dong, Yangcheon-ku, Seoul 158-710, Republic of Korea
E-mail: goodmorning@ewha.ac.kr

Key words: ovarian cancer, metastasis, mouse xenograft, *AGR2*, DNA methylation

Introduction

Ovarian cancer has the highest fatality rate among all gynecological cancers, since more than 70% of ovarian cancer patients are initially diagnosed when the cancer is in advanced stages (1,2). Although there have been significant improvements in surgical treatments and chemotherapy, the overall survival rate remains poor (3). The poor survival rate is attributed to frequent recurrence after several disease-free months, which are obtained by optimal debulking surgery and subsequent chemotherapy. Since all of the ovarian tissue is removed during standard treatment, which includes total hysterectomy with bilateral salpingo-oophorectomy, all recurrences in ovarian cancer following primary treatment are metastatic recurrences.

The complex biological process of metastasis involves molecular mechanisms of adhesion, migration, invasion, growth, proliferation and apoptosis. The pattern of metastatic dissemination in ovarian cancer is unique, differing from classical patterns of metastasis originating at other organ sites (4). Ovarian carcinoma can locally invade nearby organs, and exfoliated tumor cells can move into the intraperitoneal fluid and subsequently implant onto mesothelial surfaces, causing ascites accumulation as the peritoneal lymphatic drainage is obstructed and the tumor cells secrete vascular permeability factors (5).

DNA methylation is an important mechanism for silencing gene expression during cancer progression and metastasis (6). Cancer metastasis is a multi-step process in which the progressive accumulation of aberrant epigenetic alterations provides cancer cells with the proteins required to survive in a hostile circulatory environment and at distant anatomical sites (7).

Pro-oncogenic anterior gradient 2 (*AGR2*) gene encodes a 17-kDa protein that is conserved in vertebrates and was first identified as a secreted protein in *Xenopus laevis*, which is expressed during neural developmental processes including the formation of the forebrain and the mucus-secreting gland (8). *AGR2* was studied in cancers and is reported to be highly expressed in adenocarcinomas of the esophagus, pancreas and prostate (9-11). *AGR2* expression is upregulated in response to ER stress, and research shows that the basal expression of *AGR2* could be regulated by IRE1 and ATF6 (12).

To identify genes regulating tumor metastasis, we implanted cells of the human ovarian cancer cell line SK-OV-3 into the peritoneal cavity of mice to generate a tumor xenograft mouse model that mimics human ovarian cancer metastasis. We found that DNA methylation at CpG sites within the promoter region regulates the expression of *AGR2*, and the *AGR2* gene product enhances the aggressive phenotypes of ovarian cancer cells.

Materials and methods

Cell culture. Human ovarian cancer cell line SK-OV-3 was purchased from the American Type Culture Collection (ATCC no. HTB-77) and cultured in McCoy's 5A medium containing 10% fetal bovine serum, 100 U/ml penicillin and 100 μg/ml streptomycin (all from Gibco/BRL) in a 95% humidified air and 5% CO_2 atmosphere at 37˚C.

Ovarian cancer mouse xenograft model. All procedures for handling and euthanizing the animals used in this study were performed in strict compliance with the guidelines of the Korean Animal Protection Law and approved by the Institutional Animal Care and Use Committee (IACUC) of Ewha Woman's University School of Medicine. SK-OV-3 cells ($2x10^6$) suspended in culture media were intraperitoneally injected into 10 female nude mice (BALB/c, 4-6 weeks old). Four weeks after inoculation, the xenograft mice were sacrificed, and at least four implants adhering to the mesothelial surface of each mouse were harvested.

Messenger RNA microarray chip processing and analysis of gene expression data. Total RNA was extracted from the harvested metastatic-implant of ovarian cancer mouse xenografts and SK-OV-3 cells using the RNeasy mini kit (Qiagen), and 1 μg of total RNA was amplified and labeled according to the Affymetrix GeneChip Whole Transcript Sense Target Labeling protocol. The resulting labeled cDNA was hybridized to Affymetrix Human Gene 1.0 ST arrays (Affimetrix). The scanned raw expression values were background corrected, normalized, and summarized using the Robust Multiarray Averaging approach in the Bioconductor "affy" package (Affimetrix). The resulting $\log_2$-transformed data were used for further analyses.

To identify differentially expressed genes (DEGs), we applied moderated t-statistics based on an empirical Bayesian approach (11). Significantly upregulated and downregulated DEGs were defined as genes with at least a 2-fold difference in expression level between the xenograft cells and the wild-type SK-OV-3 cells after correction for multiple testing [Benjamini-Hochberg false-discovery rate (BH FDR)-adjusted P-value <0.05] (18). Finally, we excluded genes with a low expression level (maximum $\log_2$ expression level in a total of eight samples <7.0) from the list of DEGs. The DAVID bioinformatics resource was used to detect overrepresented GO clusters from the identified DEGs (13).

Quantitative real-time polymerase chain reaction (qRT-PCR). One microgram of total RNA was converted to complementary DNA (cDNA) using Superscript II reverse transcriptase (Invitrogen, Carlsbad, CA, USA) and oligo-$(dT)_{12-18}$ primer (Invitrogen) according to the manufacturer's standard. The qRT-PCR was performed in a 20-μl reaction mixture containing 1 μl cDNA, 10 μl SYBR Premix EX Taq (Takara Bio), 0.4 μl Rox reference dye (50X; Takara Bio) and 200 nM of primers for each gene using 7500 Fast Real-Time PCR system (Applied BioSystems). The primer sequences were as follows: *AGR2* (forward), 5'-AGTTTGTCCTCCTCAATC TGG TTT-3' and *AGR2* (reverse), 5'-GACATACTGGCCAT CAGGAGAAA-3'; GAPDH (forward), 5'-AATCCCATCAC CATCTTCCA-3' and GAPDH (reverse), 5'-TGGACTCCACG ACGTACTCA-3'. The reaction ran at 95˚C for 30 sec, followed by 40 cycles of 95˚C for 3 sec and 60˚C for 30 sec and a dissociation cycle of 95˚C for 15 sec, 60˚C for 60 sec and 95˚C for 15 sec. All PCRs were performed in triplicates and the specificity of the reaction was detected by melting curve analysis at the dissociation stage. Comparative quantification of each target gene was performed based on cycle threshold (Ct) normalized to GAPDH using the ΔΔCt method.

Quantitative methylation-specific PCR (qMSP). Bisulfite treatment of genomic DNA was performed using EpiTect Bisulfite Kit (Qiagen). Quantitative real-time MSP was carried out with bisulfite-modified genomic DNA as a template using specific primer sequences for the methylated or unmethylated forms of each gene. The following methylated/unmethylated-specific primers were used: 5'-GAGTCGGCGGTTAGGA TGC-3' (methylated forward) and 5'-GAGTCGGCGGTTA GGATGT-3' (unmethylated forward) and 5'-TTTAAAAAC AAAAAACTCTTTAACCCAAA-3' (reverse). For qMSP, 20 μl of reaction mixture containing 2 μl (10-100 ng/μl) of bisulfite-treated DNA, 10 μl of SYBR Premix EX Taq (Takara Bio), 0.4 μl of Rox reference dye (50X), and 200 nM of each primer was reacted using an 7500 Fast Real-time PCR system at 95˚C for 30 sec, and then repeated for 40 cycles (at 95˚C for 3 sec, and at 62˚C for 30 sec) for amplification. The PCR product was reacted at 95˚C for 15 sec, at 60˚C for 1 min, and at 95˚C for 15 sec to examine specificity. Methylation and unmethylation of the specific CpG site were calculated as follows (Ct represents the threshold cycle):

$$\text{Percentage of methylation} = 100/(1 + 2^{\Delta Ct\ \text{methylation} - \Delta Ct\ \text{unmethylation}})\ \%.$$

Bisulfite sequencing PCR (BSP). For bisulfite sequencing of the interesting promoter region of *AGR2*, BSP was carried out using conventional PCR in a 50 μl reaction mixture containing 10 ng of bisulfite-modified genomic DNA, 1.5 mM $MgCl_2$, 200 μM dNTP, and 1 unit Platinum Taq polymerase (Invitrogen), 1 X Platinum Taq buffer and 200 nM specific BSP forward and reverse primers of each gene. The BSP primers were designed using the MethPrimer software. For *AGR2*, the BSP product was 563 bp (position in the human GRCh37/hg19 assembly: ch7 16,844,567 - 16,845,127) and contains 8 CpGs. Sequences for the BSP primers were: 5'-TTTTATTTATTTGTTTTGTGTGAGT-3' (forward) and 5'-CCTATAAAAATTAAAATACATTATTTTAA-3' (reverse). The reaction ran at 95˚C for 5 min, followed by 30 cycles of 95˚C for 30 sec, 50-55˚C for 30 sec, 72˚C for 30 sec and a final elongation step at 72˚C for 5 min.

The BSP products were purified using the QIAquick Gel Extraction kit (Qiagen) according to the manufacturer's protocols and ligated into the yT&A cloning vector (Yeastern

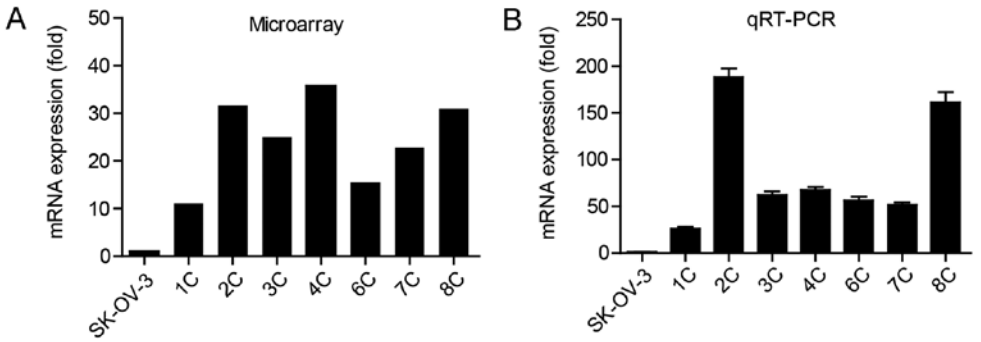

Figure 1. *AGR2* expression is upregulated in metastatic ovarian cancer implants. The transcriptional expression of *AGR2* was measured by (A) expression microarray and (B) qRT-PCR. The error bars indicate means ± SDs of triplicate experiments. The metastatic implants are labeled 1C-8C (n=7). The mRNA expression levels for each implant were normalized to values obtained for wild-type SK-OV-3 cells.

Biotech). The ligation products were used to transform competent DH5α *Escherichia coli* cells (RBC Bioscience) using standard procedures. Blue/white screening was used to select bacterial clones, and BSP product-positive clones were confirmed by colony PCR using the BSP primers to verify the insert size. Plasmid DNA was then extracted from at least 15 insert-positive clones using the QIAprep Spin Miniprep kit (Qiagen) and sequenced using the M13 primer to analyze the methylation status at specific CpG sites.

Treatment of 5-aza-2'-deoxycytidine (5-aza-dC). To demethylate the methylated CpG sites, SK-OV-3 cells were treated with increasing concentrations (0, 5, and 10 μM) of 5-aza-dC (Sigma-Aldrich) for 3 days. The medium was replaced daily.

Transient transfection. To establish a transient expression system, SK-OV-3 cells were transfected with pCMV6-XL5-*AGR2* (Origene) or pEGFP-N3 (Clontech) plasmid DNAs using Lipofectamine™ 2000 (Invitrogen). Briefly, the cells were plated at a density of $6x10^5$ cells/well in 6-well plates and allowed to grow overnight. Two micrograms of each plasmid DNA and 5 μl Lipofectamine 2000 were diluted separately in Opti-MEM medium to a total volume of 250 μl. The diluted plasmid DNAs and Lipofectamine 2000 were mixed and incubated at room temperature for 20 min to generate the transfection mixtures. The cells were washed with serum-free McCoy's 5A medium, and then the transfection mixtures were added to each well of the 6-well plates containing complete growth medium and incubated at 37˚C for 24 h in a 5% CO_2 incubator.

Transwell migration and in vitro invasion assays. After 24 h of transfection, the transfected cells were starved by serum deprivation. The cell migration assay was performed in 24-well Transwell plates containing inserts with a polycarbonate membrane with an 8.0-μm pore size (Corning). After 24 h of serum deprivation, the cells were detached from the plates and resuspended in serum-free medium at a density of $2x10^6$ cells/ml. One hundred microliters of the SK-OV-3 cell suspension was added to the upper compartment of the Transwell chamber. For each experiment, both chemotactic migration to medium containing 15% FBS and random migration in serum-free medium were assessed in parallel Transwell plates for 6 h at 37˚C in a 5% CO_2 incubator.

The *in vitro* invasion assay was performed using a BD BioCoat Matrigel Invasion Chamber (Becton-Dickinson). After 24 h of serum deprivation, SK-OV-3 cells were detached from the plates and resuspended in serum-free medium at a density of $1x10^6$ cells/ml. One hundred microliters of the SK-OV-3 cell suspension was added to the upper compartment of the invasion chamber, and 500 μl McCoy's 5A medium containing 10% FBS was added to the lower compartment of the chamber. The migration through the Matrigel chamber was allowed to proceed at 37˚C for 24 h in a 5% CO_2 incubator. After the incubation period, the cells that had not migrated from the upper side of the filter were carefully scraped away with cotton swabs. The cells on the lower side of the filter were fixed for 2 min using Diff-Quick kit solution (Fisher Scientific) stained with 1% crystal violet for 2 min and washed twice with distilled water at room temperature. The images of the stained cells on the lower side of the membrane were acquired at x200 magnification in six different fields. For quantitative analysis, the stained cells were subsequently extracted with 10% acetic acid, and colorimetric measurement was performed at 590 nm.

Results

AGR2 is highly expressed in ovarian cancer tumor tissues that metastasized from SK-OV-3 cells implanted in mice. We inoculated SK-OV-3 human ovarian cancer cells cultured *in vitro* into the perineum of female nude mice to mimic human ovarian cancer metastasis. We harvested 8 metastatic implants from 7 different mice. We then analyzed the expression profiles of the harvested cells in a microarray analysis to identify genes that were differentially expressed in the metastasized SK-OV-3 cells compared with SK-OV-3 cells cultured *in vitro*. *AGR2* expression was highly elevated in the tumor tissues, where its expression was 10- to 40-times higher than in the wild-type SK-OV-3 cells (Fig. 1A). We confirmed the upregulated *AGR2* expression in the metastatic tumor tissues by quantitative RT-PCR, which showed significantly higher expression in all of the tumor tissues (Fig. 1B) relative to the wild-type SK-OV-3 cells.

DNA methylation is reduced at CpG sites in the AGR2 promoter in the metastasized tumor tissues. We used a methylation microarray to perform global DNA methylation profiling of the 8 metastatic tumor tissues to investigate the regulatory

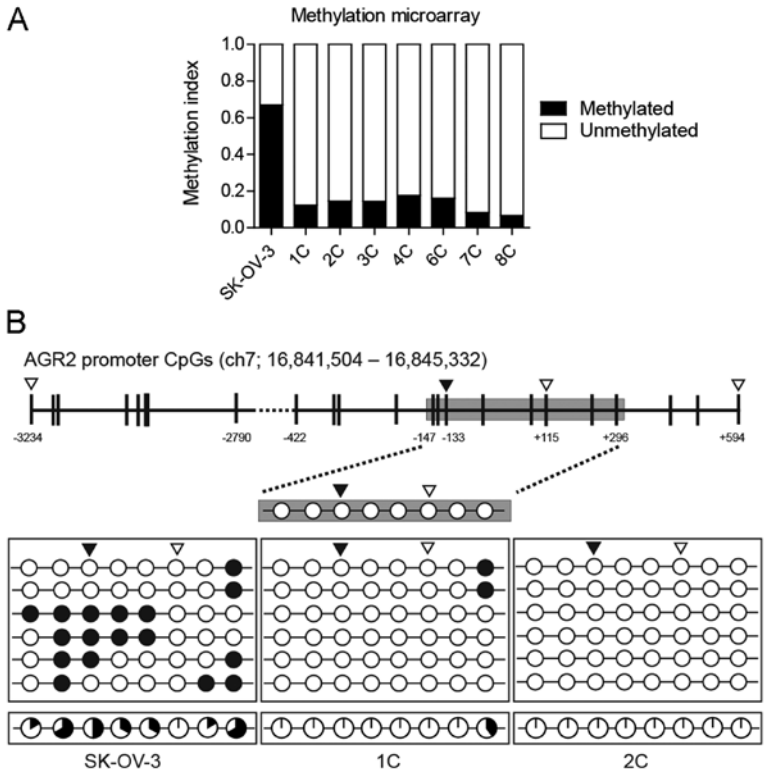

Figure 2. DNA methylation is altered at CpG sites within the *AGR2* promoter in the metastatic ovarian cancer implants. (A The DNA methylation status at specific CpG sites in the *AGR2* promoter was analyzed using the Illumina HumanMethylation450 BeadChip). Methylated, the β-value of methylated CpG; Unmethylated, the β-value of unmethylated CpG. (B) The DNA methylation status at the CpG residues in the promoter region was analyzed using Bisulfite sequencing analysis. The circles represent the methylation status of each CpG dinucleotide. The methylation status of each CpG site is illustrated by black (methylated) and white (unmethylated) circles (n=6). The percentage of methylation at each CpG site is presented in pie charts in the bottom panel. The black segment of the pie chart indicates the methylated CpG percentage, and the white segment represents the unmethylated CpG percentage. The four specific CpG sites tested in the methylation microarray are marked with triangles, and the CpG site that showed differential methylation in the methylation array is marked with a filled triangle. The promoter region of *AGR2* is located between positions 16,841,504 and 16,845,332 on chromosome 7 in the human GRCh37/hg19 assembly and contains 8 CpG residues.

mechanism underlying the abnormally high *AGR2* expression. The DNA methylation level of the CpG site at position -133 in the *AGR2* promoter was decreased more than 3-fold in all of the metastatic tumor tissues relative to the wild-type SK-OV-3 cells (Fig. 2A). We examined the status of *AGR2* promoter methylation in two metastasized tumor tissues (1C and 2C) and in the SK-OV-3 cell line. Four CpGs used in the methylation array are located in the 16,841,504 - 16,845,332 region containing the *AGR2* promoter, and only one CpG (marked in Fig. 2B with the filled triangle) showed differential methylation in the metastasized tumor tissues relative to the wild-type cells. To precisely identify the critical CpG site for enhancing *AGR2* expression, we performed bisulfite sequencing to examine 8 CpG sites between positions -147 and +296 within the *AGR2* promoter. Seven out of the 8 CpG sites were methylated in wild-type SK-OV-3 cells, whereas only one CpG site was slightly methylated in the metastasized tumor tissues, indicating that methylation at these CpG sites could regulate *AGR2* gene expression.

AGR2 expression is epigenetically modulated. We assessed the molecular mechanism of *AGR2* gene regulation using an epigenetic modulator. We treated SK-OV-3 cells with the DNA methyltransferase inhibitor 5-aza-dC to reduce the methylation status of the *AGR2* promoter. *AGR2* expression was significantly increased in a dose-dependent manner in the treated cells (Fig. 3A). We validated the methylation status in the treated cells with methylation-specific PCR using a primer set specific for the CpG at position -133 that was methylated in the microarray and bisulfite sequencing assays (Fig. 3B). Methylation of the CpG at position -133 was significantly decreased in the 5-aza-dC-treated cells in accordance with the increased expression of *AGR2*.

Overexpression of AGR2 induces aggressive phenotypes in the SK-OV-3 cells. We investigated whether *AGR2* is involved in cell migration and invasion activities. We tested the migratory ability of SK-OV-3 cells overexpressing *AGR2* and found that the upregulation of *AGR2* increased SK-OV-3 cell migration in a Transwell assay by 50% (Fig. 4). We examined the invasion of SK-OV-3 cells overexpressing *AGR2* through a Matrigel-coated membrane and found that *AGR2* overexpression significantly increased invasiveness (Fig. 5). Taken together, these results suggest that epigenetic regulation of *AGR2* confers tumor cells with migratory and invasive phenotypes.

Discussion

Metastasis is indicative of a poor prognosis for patients with ovarian cancer and most commonly occurs via the transcoelomic route, which implies intraperitoneal seeding mediated by ascites (14,15). While the molecular mechanism of metastatic

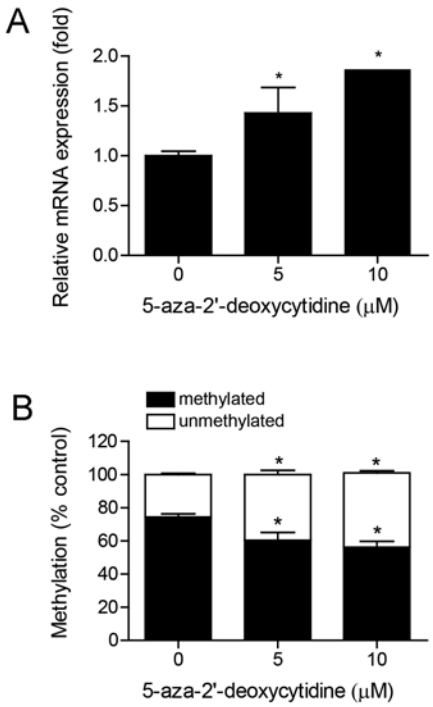

Figure 3. DNA methyltransferase inhibitor modulates *AGR2* expression in SK-OV-3 cells. SK-OV-3 cells were treated with or without the indicated concentrations of 5-aza-2'-deoxycytidine for 72 h. After treatment, (A) the expression of *AGR2* was measured by qRT-PCR, and (B) the DNA methylation status at the CpG site located at position 16,844,606 within chromosome 7 was measured using quantitative MSP. Data are shown as means ± SDs (n=3). Statistical analyses were performed using a one-way ANOVA with subsequent Bonferroni tests (*P<0.05).

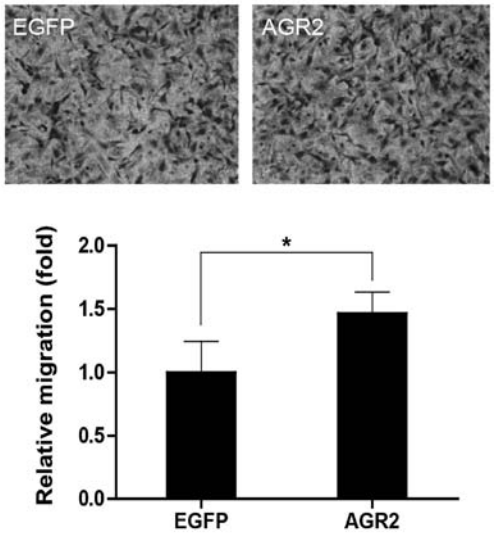

Figure 4. *AGR2* promotes migration in SK-OV-3 cells. The migratory activity of serum-starved cells towards 15% serum-containing medium was determined by a Transwell assay. Cells that migrated through a filter with 8-μm pores were fixed and stained with crystal violet. Representative images of migrated *EGFP*-transfected or *AGR2*-transfected cells are shown. The bar graph shows the relative migratory activity of the *AGR2*-overexpressing cells compared with that of the *EGFP*-expressing control cells. Quantitative analysis of the migrating cells was carried out by measuring the absorbance of crystal violet-stained cellular extracts at 595 nm. Data are shown as means ± SDs for triplicate measurements. Statistical analysis was performed using a t-test (*P<0.05).

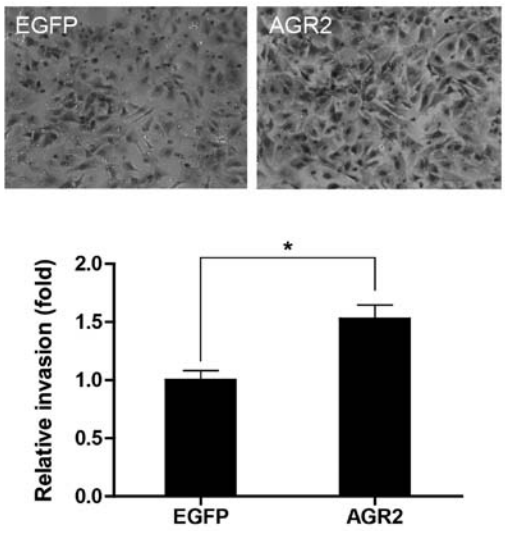

Figure 5. *AGR2* enhances the invasive activity of SK-OV-3 cells. Invasion of serum-starved cells towards 10% serum-containing medium was analyzed using a Matrigel-coated invasion chamber. The cells invading through the Matrigel were fixed and stained with crystal violet. Representative images of invading *EGFP*-transfected or *AGR2*-transfected cells are shown. Quantitative analysis of invading cells was carried out by measuring the absorbance of stained cellular extracts at 595 nm. Data are shown as means ± SDs for triplicate measurements. Statistical analysis was performed using a t-test (*P<0.05).

recurrence is not fully understood, the role of microenvironmental changes at cancer implantation sites is considered one of the central mechanisms for the intraperitoneal seeding of ovarian cancer cells (16). Among several microenvironmental factors affecting tumor aggressiveness, epigenetic alteration and consequent differential gene expression are emerging as promising new targets in the treatment of advanced ovarian cancer (17). To address the molecular mechanisms involved in ovarian cancer metastasis, we analyzed transcriptional expression levels in metastatic human ovarian carcinoma implants from mouse xenografts. The expression patterns of certain genes in our established xenograft model largely reflect the pathophysiological gene expression profiles of metastatic human ovarian cancer. The upregulated genes in our experiments were enriched with functions associated with cell adhesion, blood coagulation and wound healing, response to steroid hormone stimulus, blood vessel development and cell mobility. On the other hand, the downregulated genes were enriched with functions associated with the inflammatory response, programmed cell death and response to endoplasmic reticulum stress.

During the progression of metastasis, ovarian tumor cells exfoliate from their place of origin and attach to a new location in a process requiring the remodeling of cell-cell junctions and the alteration of adhesive properties. Our gene ontology (GO) analysis showed that *P-cadherin, cadherin 16, protocadherin 18*, and the protocadherin β cluster, all of which are involved in cell adhesion (GO terms: cell adhesion, biological adhesion, hemophilic cell adhesion, calcium-dependent cell-cell adhesion, cell-cell adhesion) were significantly upregulated in the metastatic cells. In addition to cadherin and the protocadherin family, the expression levels of certain integrin family genes (*ITGB4*, *ITGB6*, and *ITGA7*) were upregulated in our

ovarian metastatic implants. These genes encode adhesion receptors that function in signaling from the extracellular matrix to the cell. Integrin proteins form dimers composed of α and β chains, and integrin heterodimers bind to fibronectin, collagen VI, laminin and transforming growth factor 1 (*TGF1*), promoting cell growth and matrix production by providing physical adhesion between the cytoskeletal structure and the extracellular matrix (18,19).

ITGB4 levels are highly elevated in cells derived from human ovarian cancer cell lines that possess aggressive phenotypes. Immunostaining of ITGB4 in 196 human ovarian serous carcinoma samples revealed that high levels of ITGB4 are related with tumor aggressiveness (20). In accordance with a recent report of the altered expression of collagen-remodeling genes, such as *COL6A2*, that are regulated by TGF-β signaling and are associated with metastasis and poor survival in patients with serous ovarian cancer (21), the expression profile of collagen superfamily genes including *COL6A2* was extensively modified in our ovarian metastatic implants. *CXCR4* is the only chemokine receptor expressed in ovarian tumor cells (22); and the CXCR4 ligand, CXCL12, has been detected in the ascites of patients with ovarian cancer and is secreted by peritoneal mesothelial cells. The CXCR4-CXCL12 interaction could direct cancer cell migration in the peritoneum, leading to the spread of ovarian cancer (22).

We also found that S100 family members including *S100A1*, *S100A2*, *S100A3* and *S100A4* were upregulated in the metastasized tumor tissues. The overexpression of S100 family members has been described in many types of cancers, and the upregulated products of these genes promote metastasis by interacting with key molecules, including matrix metalloproteinase, and act as chemo-attractants. In particular, S100A4 has been suggested as a biomarker for identifying the high risk of metastasis and reduced survival in patients with solid tumors, including those caused by bladder cancer, breast cancer, esophageal squamous cell carcinomas, pancreatic cancer and colorectal carcinomas (23-28).

Elevated expression of *AGR2* in human cancers was previously observed in several studies (9-12). We found aberrant DNA methylation at CpG sites in the *AGR2* promoter region in metastatic ovarian cancer cells, suggesting that ovarian cancer cells obtain aggressive phenotypes for metastasis through alterations in DNA methylation profiles and subsequent gene expression. Our results demonstrated that understanding the pathophysiologic events at the epigenetic level as well as the genetic level may be an important basis for elucidating the mechanisms of ovarian cancer metastasis and recurrence.

Acknowledgements

This study was supported by a grant of the Korean Health Technology R&D Project, Ministry of Health & Welfare, Republic of Korea (HI12C0050).

References

1. Siegel R, Naishadham D and Jemal A: Cancer statistics, 2013. CA Cancer J Clin 63: 11-30, 2013.
2. Lengyel E: Ovarian cancer development and metastasis. Am J Pathol 177: 1053-1064, 2010.
3. Kipps E, Tan DS and Kaye SB: Meeting the challenge of ascites in ovarian cancer: new avenues for therapy and research. Nat Rev Cancer 13: 273-282, 2013.
4. Sale S and Orsulic S: Models of ovarian cancer metastasis: Murine models. Drug Discov Today Dis Models 3: 149-154, 2006.
5. Naora H and Montell DJ: Ovarian cancer metastasis: integrating insights from disparate model organisms. Nat Rev Cancer 5: 355-366, 2005.
6. Portela A and Esteller M: Epigenetic modifications and human disease. Nat Biotechnol 28: 1057-1068, 2010.
7. Valastyan S and Weinberg RA: Tumor metastasis: molecular insights and evolving paradigms. Cell 147: 275-292, 2011.
8. Aberger F, Weidinger G, Grunz H and Richter K: Anterior specification of embryonic ectoderm: the role of the *Xenopus* cement gland-specific gene XAG-2. Mech Dev 72: 115-130, 1998.
9. Thompson DA and Weigel RJ: hAG-2, the human homologue of the *Xenopus laevis* cement gland gene XAG-2, is coexpressed with estrogen receptor in breast cancer cell lines. Biochem Biophys Res Commun 251: 111-116, 1998.
10. Fletcher GC, Patel S, Tyson K, *et al*: hAG-2 and hAG-3, human homologues of genes involved in differentiation, are associated with oestrogen receptor-positive breast tumours and interact with metastasis gene C4.4a and dystroglycan. Br J Cancer 88: 579-585, 2003.
11. Hao Y, Triadafilopoulos G, Sahbaie P, Young HS, Omary MB and Lowe AW: Gene expression profiling reveals stromal genes expressed in common between Barrett's esophagus and adenocarcinoma. Gastroenterology 131: 925-933, 2006.
12. Higa A, Mulot A, Delom F, *et al*: Role of pro-oncogenic protein disulfide isomerase (PDI) family member anterior gradient 2 (AGR2) in the control of endoplasmic reticulum homeostasis. J Biol Chem 286: 44855-44868, 2011.
13. Huang da W, Sherman BT and Lempicki RA: Systematic and integrative analysis of large gene lists using DAVID bioinformatics resources. Nat Protoc 4: 44-57, 2009.
14. Feki A, Berardi P, Bellingan G, *et al*: Dissemination of intraperitoneal ovarian cancer: Discussion of mechanisms and demonstration of lymphatic spreading in ovarian cancer model. Crit Rev Oncol Hematol 72: 1-9, 2009.
15. Tan DS, Agarwal R and Kaye SB: Mechanisms of transcoelomic metastasis in ovarian cancer. Lancet Oncol 7: 925-934, 2006.
16. Jeon B-H, Jang C, Han J, *et al*: Profound but dysfunctional lymphangiogenesis via vascular endothelial growth factor ligands from $CD11b^+$ macrophages in advanced ovarian cancer. Cancer Res 68: 1100-1109, 2008.
17. Cock-Rada A and Weitzman JB: The methylation landscape of tumour metastasis. Biol Cell 105: 73-90, 2013.
18. Howe A, Aplin AE, Alahari SK and Juliano R: Integrin signaling and cell growth control. Curr Opin Cell Biol 10: 220-231, 1998.
19. Aplin A, Howe A, Alahari S and Juliano R: Signal transduction and signal modulation by cell adhesion receptors: the role of integrins, cadherins, immunoglobulin-cell adhesion molecules, and selectins. Pharmacol Rev 50: 197-263, 1998.
20. Choi YP, Kim BG, Gao M-Q, Kang S and Cho NH: Targeting ILK and β4 integrin abrogates the invasive potential of ovarian cancer. Biochem Biophys Res Commun 427: 642-648, 2012.
21. Cheon DJ, Tong Y, Sim MS, *et al*: A collagen-remodeling gene signature regulated by TGF-β signaling is associated with metastasis and poor survival in serous ovarian cancer. Clin Cancer Res 20: 711-723, 2013.
22. Scotton CJ, Wilson JL, Milliken D, Stamp G and Balkwill FR: Epithelial cancer cell migration: a role for chemokine receptors? Cancer Res 61: 4961-4965, 2001.
23. Salama I, Malone P, Mihaimeed F and Jones JL: A review of the S100 proteins in cancer. Eur J Surg Oncol 34: 357-364, 2008.
24. Davies BR, O'Donnell M, Durkan GC, *et al*: Expression of S100A4 protein is associated with metastasis and reduced survival in human bladder cancer. J Pathol 196: 292-299, 2002.
25. Rudland PS, Platt-Higgins A, Renshaw C, *et al*: Prognostic significance of the metastasis-inducing protein S100A4 (p9Ka) in human breast cancer. Cancer Res 60: 1595-1603, 2000.
26. Ai KX, Lu LY, Huang XY, Chen W and Zhang HZ: Prognostic significance of S100A4 and vascular endothelial growth factor expression in pancreatic cancer. World J Gastroenterol 14: 1931-1935, 2008.
27. Gongoll S, Peters G, Mengel M, *et al*: Prognostic significance of calcium-binding protein S100A4 in colorectal cancer. Gastroenterology 123: 1478-1484, 2002.
28. Ninomiya I, Ohta T, Fushida S, *et al*: Increased expression of S100A4 and its prognostic significance in esophageal squamous cell carcinoma. Int J Oncol 18: 715-720, 2001.